Pharmaceutical Research (2023) 40:2873–2886
https://doi.org/10.1007/s11095-023-03546-5

ORIGINAL RESEARCH ARTICLE

Multiphysics Simulation of Local Transport and Absorption Coupled with Pharmacokinetic Modeling of Systemic Exposure of Subcutaneously Injected Drug Solution

Clairissa D. Corpstein[1] · Peng Hou[1] · Kinam Park[1] · Tonglei Li[1]

Received: 22 March 2023 / Accepted: 2 June 2023 / Published online: 21 June 2023

Abstract

Introduction Subcutaneous (SC) injectables have become more acceptable and feasible for administration of biologics and small molecules. However, efficient development of these products is limited to costly and time-consuming techniques, partially because absorption mechanisms and kinetics at the local site of injection remain poorly understood.

Objective To bridge formulation critical quality attributes (CQA) of injectables with local physiological conditions to predict systemic exposure of these products.

Methodology We have previously developed a multiscale, multiphysics computational model to simulate lymphatic absorption and whole-body pharmacokinetics of monoclonal antibodies. The same simulation framework was applied in this study to compute the capillary absorption of solubilized small molecule drugs that are injected subcutaneously. Sensitivity analyses were conducted to probe the impact by key simulation parameters on the local and systemic exposures.

Results This framework was capable of determining which parameters had the biggest impact on small molecule absorption in the SC. Particularly, membrane permeability of a drug was found to have the biggest impact on drug absorption kinetics, followed by capillary density and drug diffusivity.

Conclusion Our modelling framework proved feasible in predicting local transport and systemic absorption from the injection site of small molecules. Understanding the effect of these properties and how to model them may help to greatly expedite the development process.

Keywords capillary absorption · CQA · FEM/CFD · injectable · subcutaneous

Introduction

The recent development of subcutaneous (SC), or fatty tissue, injectables has enabled administration of biologic drugs (e.g., insulin, monoclonal antibodies) and small molecule formulations. For the latter, long-acting injectables (LAI) are being actively pursued to treat chronic diseases because of the avoidance of first-pass metabolism and improved patient compliance. Design of SC injectable products can be optimized to control local release and absorption rate kinetics by understanding critical quality attributes (CQAs) for drug formulations as well as the complex physiological space. The SC is mainly comprised of extracellular matrix (ECM), adipose tissue, and an active immune cell environment. This physiology provides structural integrity and hydration to the skin, energy metabolism and temperature regulation, and defense against foreign particles or organisms [1, 2]. Because of the porous structure, the ECM also permits diffusive control of administered drug molecules or drug delivery vehicles [2]. The presence of lymphatic vessels, in addition to capillary, facilitates immune trafficking of drug delivery vehicles to lymph nodes or into the mononuclear phagocytic system organs (MPS), such as the liver [3].

Despite the interest and benefit that SC injectables have for patients, translation of formulation designs into the clinic is slowed by a lack of understanding regarding unique absorption mechanisms from the SC injection site into the systemic circulation. The same physiological complexity that offers many advantages to drug delivery cannot be fully comprehended during preclinical testing, making

✉ Tonglei Li
tonglei@purdue.edu

[1] Department of Industrial and Physical Pharmacy, Purdue University, 525 Stadium Mall Dr. RHPH Building, West Lafayette, Indiana, IN 47907, USA

the extrapolation of systemic exposure in humans from preclinical drug release kinetics nearly impossible to do. This limits development of novel SC injectables to costly and time-consuming trial-and-error techniques, and development of generics to inefficient explorations designed for oral drugs (including *in vitro – in vivo* correlations, or IVIVC). For drugs with complex formulations (e.g., drug delivery vehicles, pro-drugs, etc.) that can impact SC absorption rates, using IVIVC data as a substitute for clinical trials is not feasible because of potential interplays between CQAs and local physiological conditions. For drugs that are physiology (e.g., permeability) rate limited, IVIVC are difficult to develop because of the complications in predicting the physiological effect on absorption rates. Implementation of computational methods can therefore be useful in overcoming these limitations in preclinical testing by describing the relationships between the SC space and injected formulations on absorption mechanisms in a way that is both discriminating and mechanistic.

The increase in and growing accessibility of computational software has allowed for application of modeling and simulation to revolutionize all stages of pharmaceutical development, ranging from using Quantitative Structure-Property or -Activity Relationships (QSPR/QSAR) to screen for drug-like molecules, utilizing molecular dynamics (MD) simulations to probe protein stability, and to integrating the discrete element method (DEM) with computational fluid dynamics (CFD) to understand powder flow during manufacturing [4]. Physiologically based pharmacokinetic (PBPK) models have also gained considerable traction for a variety of applications, such as to inform design of *in vitro* release experiments [5, 6], predict dose requirements [4], and substitute for bioequivalence studies [7, 8]. Nevertheless, there remains a critical need to integrate simulations for subcutaneous (SC) specific absorption rate mechanisms and systemic pharmacokinetics. It is especially necessary to correlate changes in formulation to changes in PK profiles, which cannot be reliably predicted by *in vitro* testing of the product. By understanding SC absorption mechanisms to bridge formulation CQAs and directly test their effects on pharmacokinetics, computational methods can be used to guide and support preclinical testing. It has been a main research goal of ours to integrate CFD-based simulations of the SC space with whole-body PK modeling to guide the development of SC formulation design. This integration allows for concurrent testing of parameters and complex relationships between both the subcutaneous physiological environment and the injected drug physicochemical and formulation properties. Ultimately, this methodology is expected to bridge the gap between preclinical and clinical data to help predict *in vivo* injectable performance from *in vitro* data.

We have previously developed a CFD/FEM absorption model framework for monoclonal antibody (mAb) absorption into the lymphatics [9-11]. When integrated with a minimal-PBPK (mPBPK) model for lymphatic absorption and disposition, simulated pharmacokinetic profiles of different mAb drugs were validated against experimental pharmacokinetics. Herein, application of the model framework has been expanded to include blood capillary absorption of a small molecule solution formulation (methotrexate, MTX). Sensitivity analyses of physiological and drug parameters were conducted via simulation to understand the effect and relevance of these parameters on drug exposure using compartmental pharmacokinetic modeling. Overall, blood absorption of small molecule drugs administered in the subcutaneous was successfully implemented, allowing for an understanding of significant absorption rate parameters and their effect on drug plasma concentrations in humans.

Experimental Procedures

Our simulation and modeling framework integrates the finite element method (FEM) to solve a CFD model of local transport and absorption of an SC administered formulation with compartmental-based PK modeling of systemic exposure. This framework was derived from our earlier studies of simulating locally administered mAbs using COMSOL Multiphysics ver. 5.3 (COMSOL Inc., MA, USA)) [9-11]. The local model treats the SC space as a homogenous, poroelastic media, where tissue is considered compressible, and the interstitial fluid is taken as non-compressible and isothermal. Fluid flow is modeled using Darcy's Law [9]. Mass transport of drug is subject to both advection (due to injection) and diffusion in the porous media and across vessel membranes. Changes in tissue deformation, fluid velocity, and mass transport were coupled with changes in porosity and permeability of the tissue as drug is injected into the tissue space and subsequently absorbed. Upon tissue recovery from injection-induced deformation, drug absorption is primarily determined by membrane permeability as well as diffusion gradients in the SC.

Local Simulation – Mass Transport of Drug Molecules

The interplay between the SC space and lymphatic and capillary vessels impacts fluid flow and mass transport of drug [12]. As blood is pumped through blood vessels, convective forces push excess interstitial fluid – and any foreign particles, debris, or pathogens in the blood – into the lymphatics. Cleaned interstitial fluid is then returned to blood vessels of low flow rate (e.g., veins). Capillaries are primarily responsible for the transport of small drug molecules from tissues into the blood [13]. The movement of fluid is maintained by a balance of four pressures – tissue and vessel (hydrostatic), and interstitial and vessel osmotic pressures (oncotic) – and

is often modeled by the Starling equation described below [12]. Differing from our previous studies of mAbs where only lymphatic absorption was considered, small molecule drug absorption occurs into the capillaries. Therefore, lymphatic parameters were replaced to describe capillary properties. Mass transport of drug in the interstitial space is calculated using the diffusion-advection equation below:

$$\frac{\partial(\varnothing c)}{\partial t} + \left(D_{eff}\nabla c\right) + \nabla \cdot \left(c\vec{v}\right) = Q_{bl} = -P_a c\frac{S}{V} \tag{1}$$

where the terms on the left side describe drug concentration (c) with respect to tissue porosity ($\varnothing$) as a function of time, and under the influence of diffusive (D_{eff}) and advective ($\vec{v}$) forces. The term on the right side (Q_{bl}) describes the sink condition, or absorption into blood, which is determined by apparent permeability (P_a), drug concentration (c), and the surface area of vessels per volume of tissue ($\frac{S}{V}$). P_a characterizes the contributions of membrane permeability and fluid flux to drug permeability into a blood vessel, and is described by the Starling equation below:

$$P_a = P_d\left(\frac{P_e}{e^{P_e}-1}\right) + \left\{L_p(1-\gamma)\left(\left(p-p_{bl}\right)+\gamma\left(\pi-\pi_{bl}\right)\right)\right\} \tag{2}$$

where P_d is the membrane diffusive permeability; P_e is the Peclet number, which represents the ratio of advection vs. diffusion; L_p is the hydraulic conductivity, which measures how fast water passes across the membrane; γ is the drug reflection coefficient, which approximates the percentage of drug reflected back from a membrane pore; p is the interstitial fluid pressure; p_{bl} is the vessel pressure; π is the interstitial osmotic pressure; and π_{bl} is the capillary osmotic pressure. The Peclet number can be calculated below:

$$P_e = \frac{L_p(1-\gamma)\left(\left(p-p_{bl}\right)+\gamma\left(\pi-\pi_{bl}\right)\right)}{P_d} \tag{3}$$

where the term $\gamma(\pi-\pi_{bl})$ represents fluid flux based on differences in fluid and colloid oncotic pressures due to protein concentrations in the SC and vessels. Table I shows the capillary vessel physiological conditions.

Table I Physiological Parameters of Capillary Vessels in the Subcutaneous Tissue

Parameter	Value	Measurement Condition	Ref.
S/V (1/cm)	0.3	Estimated based on the number of blood vessels in human SC tissue and assuming cylindrical vessels	[14]
L_p (cm/Pa*s)	4×10^{-9}	Measured with HUVEC monolayers *in vitro*	[15]
P_{bl} (Pa)	1133	Measured *in vivo* in human SC (trunk)	[16]
π (Pa)	2026	Measured *in vivo* in human SC (trunk)	[16]
π_{bl} (Pa)	3840	Measured *in vivo* in human SC (trunk)	[16]

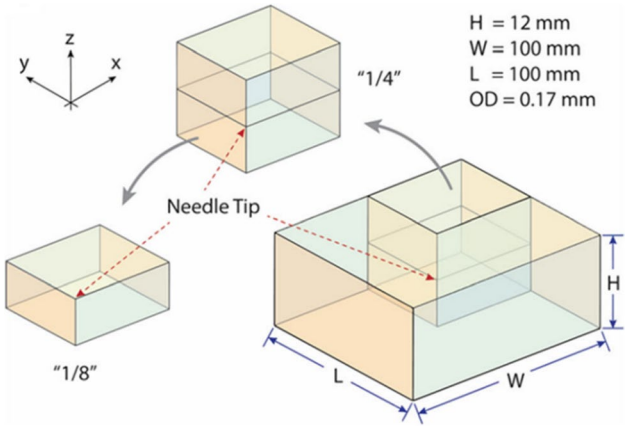

Fig. 1 Model space overview. Visual description of modeling space. Injection occurs at needle tip (center of model). Graphics of changes in model space utilizes different quadrants for better visualization. (Adopted from [9]).

Figure 1 illustrates the configuration of the local simulation model. For this study, a "1/4" model was 5 x 5 x 12 mm^3, and a "1/8" model was 5 x 5 x 6 mm^3. The injection process was firstly simulated, long enough for the total drug dose to be deposited into the modelling space. The absorption process was then computed using the physiological conditions and drug concentrations obtained at the end of the injection process. Finally, the rate of drug absorption was inputted into compartmental pharmacokinetics in order to simulate plasma concentration profiles. In this study, solubilized methotrexate (MTX) was chosen as the model delivery system. Its physicochemical properties, specifically membrane permeability and tissue diffusion, were available in literature. Moreover, both intravenous (IV) and subcutaneous (SC) pharmacokinetic studies were available to validate the model.

Pertinent physicochemical properties of MTX are listed in Table II. Estimations for reflection coefficient were calculated using molecular volume and the drug's octanol-water partition coefficient [17]. Sensitivity analyses of both drug physicochemical and SC physiological properties were conducted using the simulation model. The effect of vessel physiology and tissue diffusion rates were measured when membrane permeability was both low (6×10^{-8} cm/s) and high (3.5×10^{-5} cm/s). Additionally, blood pressure and hydraulic conductivity have been linked *in vitro*, where an increase in transmural vessel pressure decreased hydraulic conductivity, and an increase in shear stress increased it [18, 19]. Therefore, the combined effects of changing both these parameters were also determined.

PK Modeling of Systemic Exposure

Compartmental modeling was used to calculate the whole-body pharmacokinetic profile of SC injected methotrexate

Table II Physicochemical Properties of Methotrexate

Parameter	Value	Measurement Condition	Ref.
P_d (cm/s)	6×10^{-8}	Measured by *in vitro* PAMPA model	[20]
D_{eff} (cm^2/s)	2.47×10^{-6}	Measured with ex vivo mouse epidermis	[21, 22]
γ	7×10^{-4}	*Est.*	[17]
Dose/Volume	7.5 mg/0.15 mL 15 mg/0.30 mL 22.5 mg/0.45 mL 30 mg/0.60 mL	Human SC autoinjector	[23]
Inj. Rate	0.08 mL/s	*Est.*	[9]
Inj. Time	2.6 s	*Est.*	–
L x W (cm)	10×10	*Est.*	–

that was computed by the FEM model. The simulated local drug concentration profiles were fitted to first-order kinetics to determine the absorption rate (k_a):

$$M_{drug} = Dose * e^{-k_a t} \tag{4}$$

where M_{drug} is the mass of drug, dose is the administered initial mass of drug, k_a is the absorption rate, and t is time. Model fitting was done using OriginPro 2022 (OriginLab, MA, USA). Intravenous (IV) data [14, 24] was used to derive PK parameters of the compartmental model in SimBiology (MATLAB R2020a, MathWorks Inc., MA, USA) for methotrexate, including clearance and volume of distribution. A 1-compartment model was developed for methotrexate. Figure 2 shows a description of the compartmental model used. Table III shows the pharmacokinetic parameters.

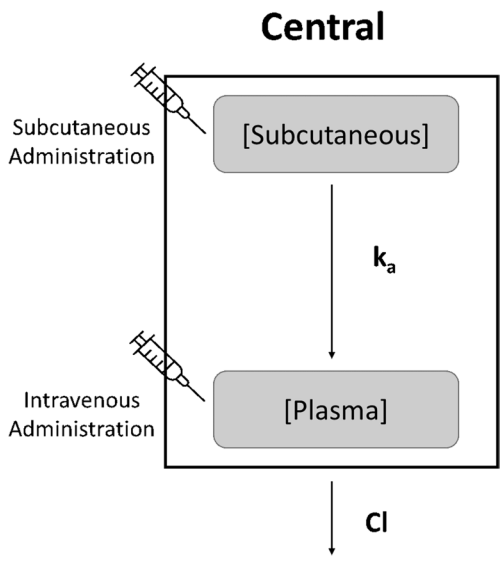

Fig. 2 Pharmacokinetic model overview. Visual description of compartmental model used for methotrexate.

Concentration kinetics in each sub-compartment (subcutaneous or plasma) was calculated with the following ordinary differential equations (ODEs):

$$\frac{d(c_{SC})}{dt} = \frac{1}{V_d} \times \left(-\left|(k_a * c_{SC}) \times V_d\right|\right) \tag{5}$$

$$\frac{d(c_{plasma})}{dt} = \frac{1}{V_d} \times \left(\left|(k_a \times c_{sc}) \times V_d\right| - \left|(k_e \times c_{plasma}) \times V_d\right|\right) \tag{6}$$

Where c_{sc} is the concentration of drug in the subcutaneous compartment, V_d is the volume of distribution, k_a is the absorption rate, c_{plasma} is the concentration of drug in the plasma compartment, and k_e is the elimination rate from the body.

To compare the goodness of fit between experimental and simulated pharmacokinetic profiles, the normalized root mean square error (NRMSE) was used:

$$NRMSE = \frac{\sqrt{\frac{\sum_{i=1}^{n}\left(X_{obs,i}-X_{model,i}\right)^2}{n}}}{\overline{X}} \tag{7}$$

where $x_{obs,i}$ and $x_{model,i}$ are the experimentally observed and model values at $time = i$, n is the number of samples, and $\overline{X}$ is

Table III Pharmacokinetic Parameters for IV and SC Methotrexate

Parameter	Value	Ref.
CL (L/h)	10	Fitted from [24] using an average weight of 71 kg
V_d (L) - central	3.8	
IV Dose (mg)	10	[24]
SC Dose (mg)	7.5 15 22.5 30	[25]

the observation mean value. Lower NRMSE values indicate better fitting between the observed and model data; higher values indicate worse fitting between the data sets.

Results

Absorption simulations for SC administration of methotrexate (MTX) were conducted to understand the impact of local physiological and drug physicochemical properties on subsequent pharmacokinetic profiles. Sensitivity analyses for these properties were used to understand the model's response to these parameters, and which had the biggest impact on the systemic exposure of SC-injected MTX. Absorption rates (k_a) obtained by the local CFD simulation were then integrated into compartmental pharmacokinetic models. Simulated plasma concentration profiles using results obtained from the sensitivity analyses showed the effect each parameter ultimately had on pharmacokinetics. This study supports the ability of our modeling framework to describe SC blood absorption of small molecule liquid formulations, and sheds light into how this framework can be used to bridge *in vitro* measured properties to *in vivo* performance of SC delivery systems.

Local Simulation of Physiological Changes in Response to SC Injection

Two consecutive studies were run to simulate the injection and absorption process of drug administered into the SC space. Figures 3 and 4 show changes in different SC tissue parameters during the drug injection ($t_{inj} = 2.6$ s) and absorption ($t_{ab} = 16$ h) phases, respectively. These parameters include tissue displacement, interstitial fluid pressure, and interstitial fluid velocity. As drug was injected, an increase in these tissue parameters was observed up to 50% of the injection time. Very little change is seen from 50% to 100% of the injection time. Tissue properties re-equilibrated very quickly after the injection was completed, effectively returning to normal in less than a second. No significant changes were observed in these variables during the sensitivity analyses conducted and described below (results not shown). It was concluded that changes in drug and blood vessel physiological properties did not impact the changes of the SC tissue before and after injection. Additionally, the effect of advection on small molecule drug absorption was also determined to be negligible. Such conclusions are reached based on the model assumption of poroelasticity of the SC tissue.

Local Simulation of MTX Drug Absorption

Figure 5 shows volume charts which represent the drug concentration evolution in the SC space during drug injection (Fig. 5A) and absorption (Fig. 5B). Absorption was simulated for 16 hours per pharmacokinetic studies conducted in literature [23]. Concentration increased during the injection process, and as absorption was initiated, also appeared to decrease over time at the injection site. However, rather than be absorbed, drug instead diffused out into the modelling space. Figure 6 supports this observation with graphs showing the integrated mass of drug (Fig. 6A) as well as radial diffusion, or cutline graphs, of drug concentration around

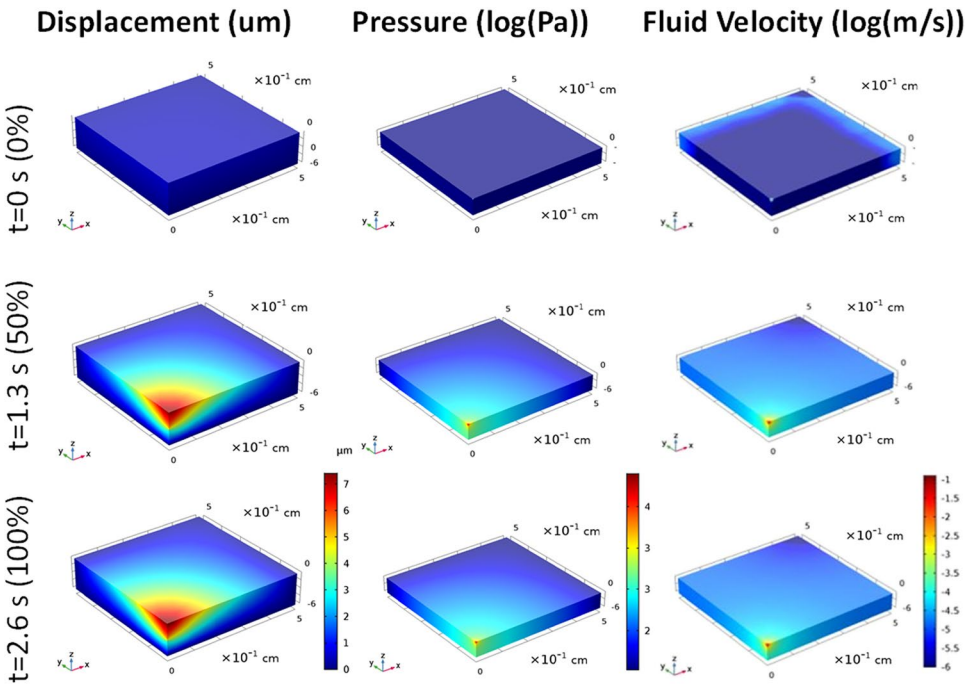

Fig. 3 Volume charts for physiological changes in SC tissue during injection. Spatial evolution of three different physiological parameters (displacement, interstitial fluid pressure, and fluid velocity) in the SC space throughout the injection period (0%, 50%, and 100% of completed injection). Displacement is depicted with a ¼ model; fluid pressure and velocity are depicted with a 1/8 model.

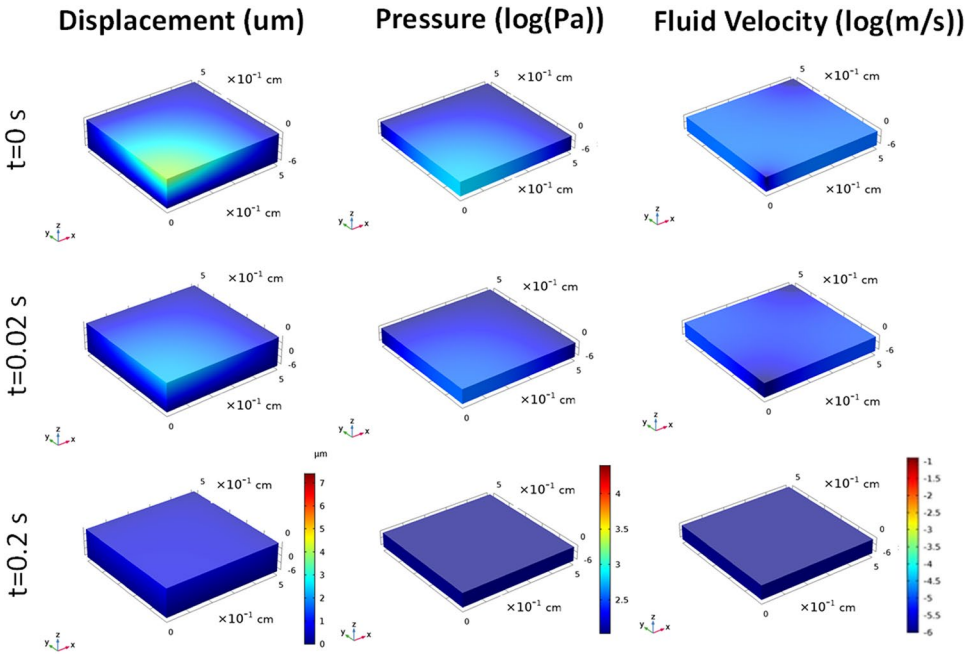

Fig. 4 Volume charts for physiological changes in SC tissue during absorption. Spatial evolution of three different physiological parameters (displacement, interstitial fluid pressure, and fluid velocity) in the SC space throughout the absorption process. Displacement is depicted with a ¼ model; fluid pressure and velocity are depicted with a 1/8 model.

the injection site (Fig. 6B). Negligible absorption (<1%) was observed (Fig. 6A), where at 16 hours, drug concentration has decreased at the injection site but diffused out radially into the rest of the model (Fig. 6B). Therefore, the absorption rate was very low. Because of this, sensitivity analyses of low, medium, and high parameter values were conducted for drug (e.g., membrane permeability, diffusion rates, and reflection coefficient) and blood vessel physiology (e.g., capillary surface area, hydraulic conductivity, and vessel pressure) properties to ascertain which the model was most sensitive to, and subsequently which was most likely to impact the absorption kinetics.

Sensitivity Analysis of Local Simulation Parameters

A sensitivity analysis of drug properties showed that changes in membrane permeability had the greatest effect on absorption rate. Low to high values for sensitivity parameters were

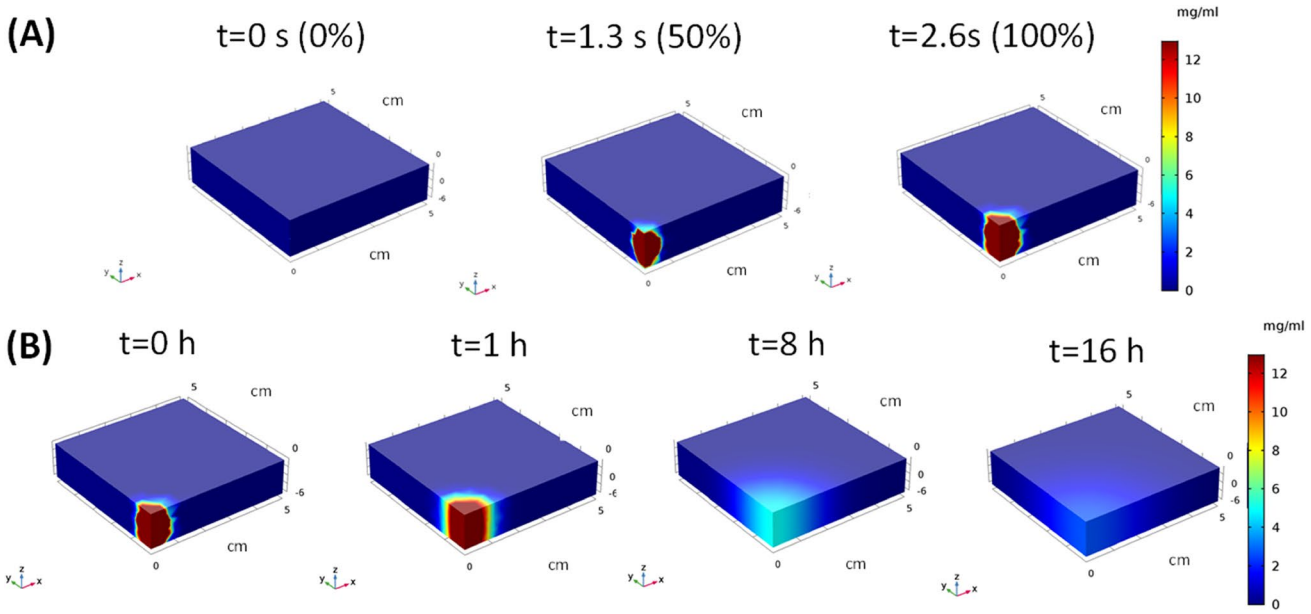

Fig. 5 Volume charts showing evolution of concentration of 7.5 mg SC dose for (**A**) injection process and (**B**) absorption process at MTX at a membrane permeability of 6×10^{-8} cm/s.

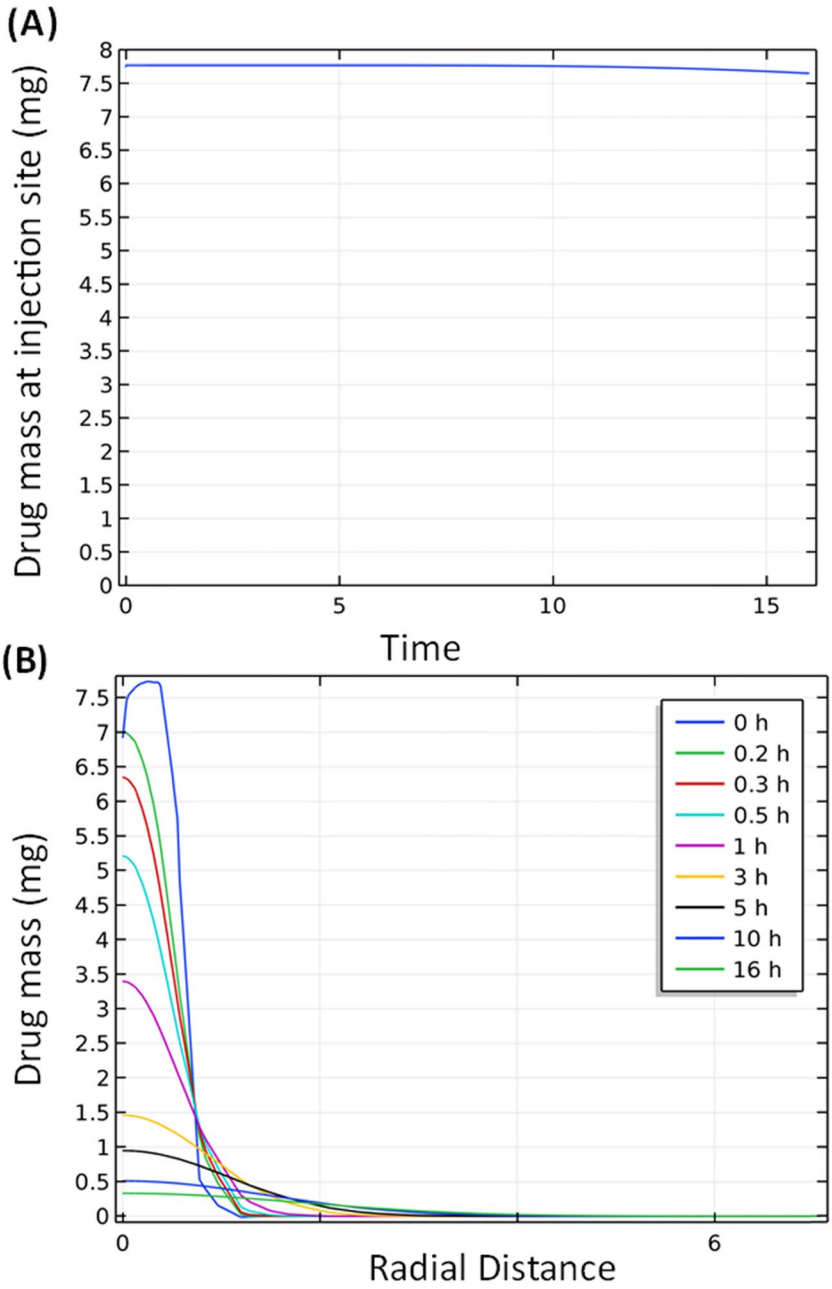

Fig. 6 MTX mass and distribution in the SC space. (**A**) integrated graphs of drug mass over time, and (**B**) Cutline graphs for radial concentration. Cutline graphs show the mass of drug as it diffuses and/or is absorbed away from the injection site (radial distance).

chosen in some cases from experimental ranges, and in others as ways to explore the extent to which a general increase or decrease of a parameter would have on absorption rates. For membrane permeability, the selected values ranged from PAMPA measured permeability to a value slightly higher than what was computationally fit in a semi-mechanistic physiologically based pharmacokinetic study [20, 24]. For diffusion rate, a range similar to membrane permeability was chosen so that magnitude and therefore effect of both drug-related properties could be more easily compared. Sensitivity analyses for vessel pressure and hydraulic conductivity compared capillary parameters to lymphatic parameters in our previous study (P_{ly} – 0 Pa, L_p – $\times 10^{-8}$ cm/(Pa*s)) [9], with an additional lower or higher value to identify a trend. Finally, capillary surface area values were chosen to find the operational range in the absence of other experimental data. The lymphatic value used in our previous study of 2 cm^{-1} was deemed too high for these purposes. At low, medium, and high permeability rates (6×10^{-8} cm/s, 6×10^{-6} cm/s, and 6×10^{-4} cm/s, respectively), k_a was calculated to be 0, 0.052, and 5.62 1/h. Changes in diffusion rate (measured at 3×10^{-8} cm^2/s, 3×10^{-6} cm^2/s, and 3×10^{-4} cm^2/s) had negligible effect on absorption rate at low permeability, except when diffusion was high (3×10^{-4} cm^2/s), which increased k_a from 0 to 0.113 1/h. However, fitting this condition to first-order kinetics was sub-optimal. The effect of reflection

Table IV Effect of Membrane Permeability and Diffusivity on Drug Absorption Rate

		P_d (cm/s)		
		$\mathbf{6\times10^{-8}}$	$\mathbf{6\times10^{-6}}$	$\mathbf{6\times10^{-4}}$
D_{eff} (cm^2/s)	$\mathbf{3\times10^{-8}}$	0	0.0371	5.62
	$\mathbf{3\times10^{-6}}$	0 ±	0.0371	5.62
	$\mathbf{3\times10^{-4}}$	0.113 *	0.155*	5.62

Bold text represent the sensitivity analysis values used for both Pd and Deff

± Baseline parameter values from literature

* Poor fitting to first-order kinetics

coefficient (γ in Eq. 2) was also studied at values of 0.0005, 0.05, and 0.1. This property represents the percent chance of a particle reflecting off the vessel membrane rather than permeating across. It is often measured for protein therapeutics or biologics; however, for small molecules, it is not readily available in literature. Estimations of reflection coefficient, dependent on molecular volume and vessel pore size, generally yield very small values [17, 26]. Nonetheless, sensitivity analyses of the reflection coefficient from 0.0005 (estimation) to literature values obtained for sugar (< 0.1) [26], showed no effect on absorption rates at low membrane permeability rates.

The relationship between membrane permeability and diffusion rates were also conducted (Table IV). The condition marked with ± ($P_d = 6\times10^{-8}$ cm/s, $D_{eff} = 3\times10^{-6}$ cm^2/s) represents the baseline parameter values obtained from literature. Starred values (*) represent those that exhibited poor fitting to first-order kinetics. Membrane permeability was, once again, found to have the biggest impact on SC absorption rates, where diffusion rate had an almost negligible effect except when diffusion rate and permeability were both high. This relationship between membrane permeability and diffusion rate could be explained by concentration gradients. At low permeability (subsequently low sink condition), absorption rates increase when the diffusion rate allows for drug to move past local saturation. At high permeability, drug is being absorbed so quickly that changes in diffusion rate have no effect.

Changes in capillary vessel physiological parameters were also found to have a negligible effect on absorption rates when membrane permeability was low. The only condition where a non-zero k_a was calculated (0.113 1/h) was at low capillary blood pressure (0 Pa), which is comparable to lymphatic vessel pressure. Sensitivity analysis to probe the relationship between hydraulic conductivity and blood pressure showed that the only conditions where k_a was measured to be non-zero was at low pressure (0 Pa) and moderate – high hydraulic conductivity (1×10^{-9} and 1×10^{-8} cm/(Pa*s), respectively). The k_a values were 0.0041 and 0.038

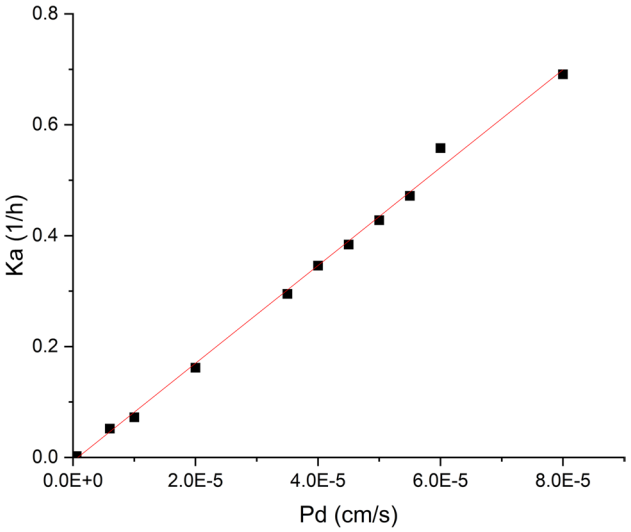

Fig. 7 Effect of Membrane Permeability on MTX absorption rate (k_a). Membrane permeability shown here was tested from 6×10^{-8} to 8×10^{-5} cm/s.

1/h, respectively, with both conditions exhibiting poor fitting to first-order kinetics. Therefore, at such a low membrane permeability value only lymphatic vessel conditions resulted in measurable absorption rates. Membrane permeability was thereby concluded to have the biggest impact on solubilized drug absorption in the SC. A sensitivity analysis was then performed to determine the relationship between membrane permeability and absorption rate (Fig. 7). The connection can be understood when looking at Eqs. 1, 2, and 4, where the sink condition (Q_{bl}) is the time derivative of the absorbed drug mass. For a small value of k_a, the derivative of Eq. 4 is roughly linear to k_a.

Values of k_a for respective permeability values were then inputted into a 1-compartmental pharmacokinetic model, and simulated plasma drug concentration profiles were compared to experimental drug concentrations in humans (Fig. 8A). K_a values associated with low permeability rate as defined by the Biopharmaceutical Classification system (BCS) – that is, a rate less than 6×10^{-6} cm/s [27] – showed negligible to nearly negligible drug plasma concentrations. At permeability rate = 1×10^{-5} cm/s, plasma concentrations increased dramatically, with a rate of 3.5×10^{-5} cm/s (brown line) best representing experimental data (black circles). Using this value to simulate plasma concentration profiles for different dose studies of 7.5, 15, 22.5, and 30 mg of MTX gave profiles that were comparable to these experimentally determined profiles (Fig. 8B). Error analysis of model fitting to the experimental data was conducted using NRMSE, which calculated the errors for these doses to be 0.066, 0.158, 0.185, and 0.310, respectively. Since the value of these errors are below 1, they suggest that the current models for SC absorption and pharmacokinetics are

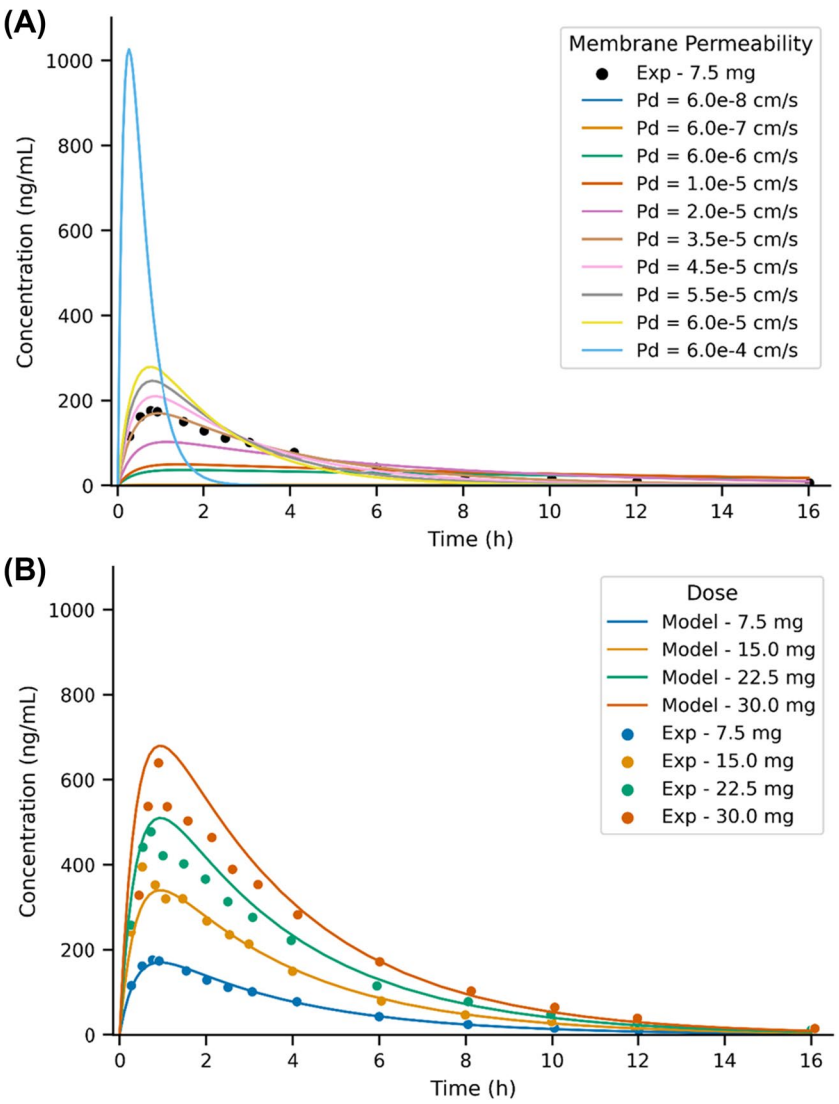

Fig. 8 – Pharmacokinetic analysis for MTX simulations. (**A**) Effect of membrane permeability on pharmacokinetic plasma concentration profiles at MTX SC dose of 7.5 mg. (**B**) Pharmacokinetic profiles of SC MTX when given at different doses experimentally (circles) and model (curve) determined, at a P_d value of 3.5×10^{-5} cm/s.

appropriate to describe plasma concentration profiles for SC administered MTX.

Figure 9 shows volume charts of MTX during the injection and absorption processes at permeability = 3.5×10^{-5} cm/s. Unlike in Fig. 5B, where drug can be seen to diffuse out into the space, Fig. 9B shows drug being eliminated from the model space. Fig. 10 further supports this by showing how the integrated mass of drug significantly decreases in comparison to what is seen in Fig. 6A. Radial diffusion graphs (Fig. 6B) also show how drug concentration is completely absorbed across the modelling space by 16 hours. Ultimately, these results show that a membrane permeability of 3.5×10^{-5} cm/s describes SC absorption and plasma concentrations better than the experimentally determined value of 6×10^{-8} cm/s. Further support for the appropriateness of such a high fitted permeability rate, compared to experimentally determined PAMPA values, may be seen in other computational models. A recently reported physiologically based pharmacokinetic (PBPK) model to describe MTX disposition in joints after oral administration fitted an oral apparent permeability (P_a) value to 6.5×10^{-5} cm/s [24]. Since MTX is a folate receptor ligand, the comparable fitted permeability values between the reported PBPK and our modelling framework may be attributed to receptor-mediated transport, rather than the passive permeability mechanism that was measured using *in vitro* PAMPA models. This also suggests the presence of folate receptors in SC capillaries, since capillary vessels are responsible for the absorption of nutrients from the skin [13, 28]. Thus, the current model fitted membrane permeability is an adequate representation of *in vivo* permeability of MTX. Because membrane permeability was determined to have the biggest effect on absorption rates, the values of the blood vessel physiological parameters were deemed appropriate to describe the average SC space. However, further sensitivity analyses were performed to determine whether changes in vessel physiology

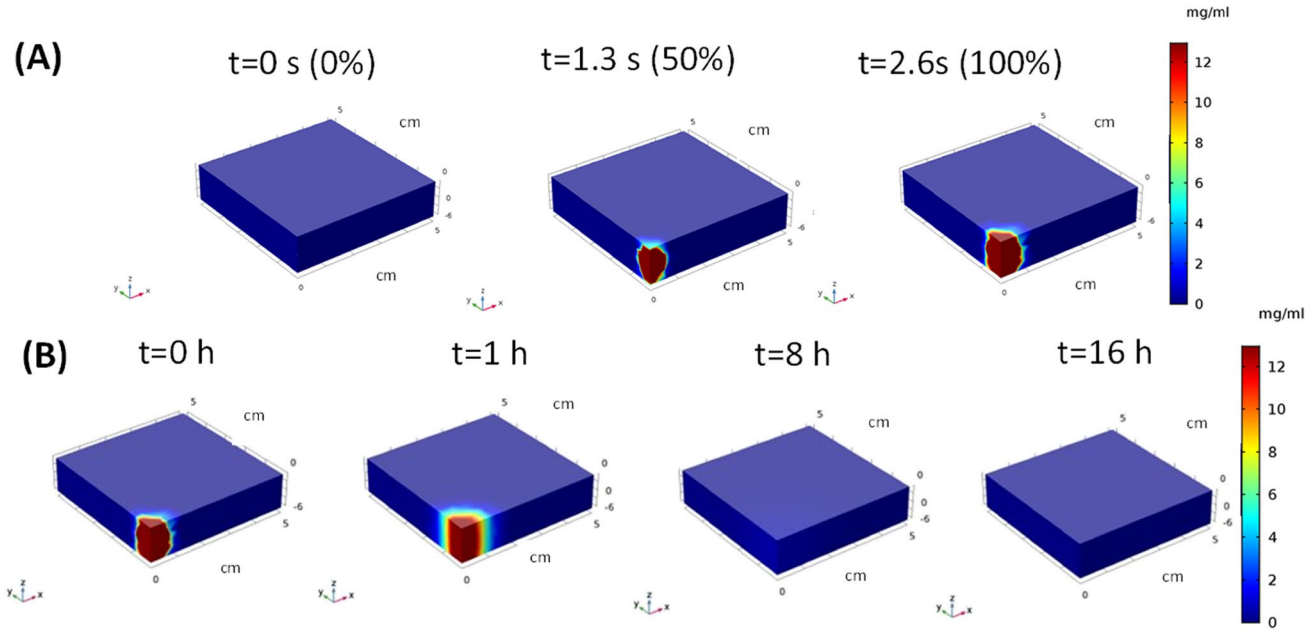

Fig. 9 Volume charts showing evolution of concentration of 7.5 mg SC dose for (**A**) injection process and (**B**) absorption process at MTX at a membrane permeability of 3.5×10^{-5} cm/s.

would have a greater impact on drug absorption rates when membrane permeability was high.

Sensitivity Analysis of Capillary Parameters and Diffusion Rates at High Permeability

When developing *in vitro* and *in vivo* correlations (IVIVC) for new drug formulations, it is often assumed that drug and formulation properties have the predominant effect on plasma concentration profiles over local physiology. Our current results show that at low injection volumes, transient perturbations in the SC – such as tissue deformation and fluid flow – have a negligible effect on absorption rates of solubilized drug. However, changes in capillary properties or ECM integrity (such as local scarring, inflammation, or age-related degradation) [29, 30] due to inter- or intrapatient variability, disease state, or special populations may serve to complicate IVIVC development. Therefore, it is important to understand the relationship between solubilized drug and SC physiological properties, and how they ultimately affect systemic plasma concentration profiles. As such, a sensitivity analysis probing the impact of surface area, pressure, and hydraulic conductivity on k_a at high membrane permeability (3.5×10^{-5} cm/s) showed that the former had the biggest impact, followed by hydraulic conductivity and pressure. A linear relationship was once again observed between changes in these parameters and ka values (results not shown). This indicates that with a few experimental values, trends could be developed using absorption rate simulations to predict the effect of untested parameters on drug absorption.

Figure 11 shows the effect of these parameters on simulated plasma concentration profiles, which had a more marked effect than the same changes in these parameters at low membrane permeability. Figure 11BC show that increases in hydraulic conductivity and pressure resulted in a decrease in absorption rate due to pressure differentials between the interstitial space and vessels (Eq. 2). This gradient means that at a high capillary vessel pressure (1133 Pa) and a low interstitial tissue pressure (~106 Pa), the pressure gradient favors fluid out of capillary vessels. In fact, at steady state conditions, fluid resorption does not happen across capillary membranes but elsewhere in the vessel hierarchy [13, 28]. However, the effect of these changes had a minimal impact on plasma concentration profiles (Fig. 12B and C), with a high hydraulic conductivity (1×10^{-8} cm/(Pa*s)) having a more significant effect than any other condition.

Studies have also shown that changes in hydraulic conductivity and vessel pressure may be related *in vitro*. One study showed that the vessel's response to an increase in the transmural pressure gradient (across the vessel membrane) was a 3x decrease in hydraulic conductivity [18]. Another study showed that shear stress (parallel to the vessel membrane) increased hydraulic conductivity [19]. Therefore, the relationship between these two variables and their effect on absorption rates was probed (Table V). At low pressure (0 Pa), the trend for hydraulic conductivity changed, that is, as hydraulic conductivity increased the absorption rate also increased. At high pressure (2000 Pa) the absorption rate decreased dramatically as hydraulic conductivity increased.

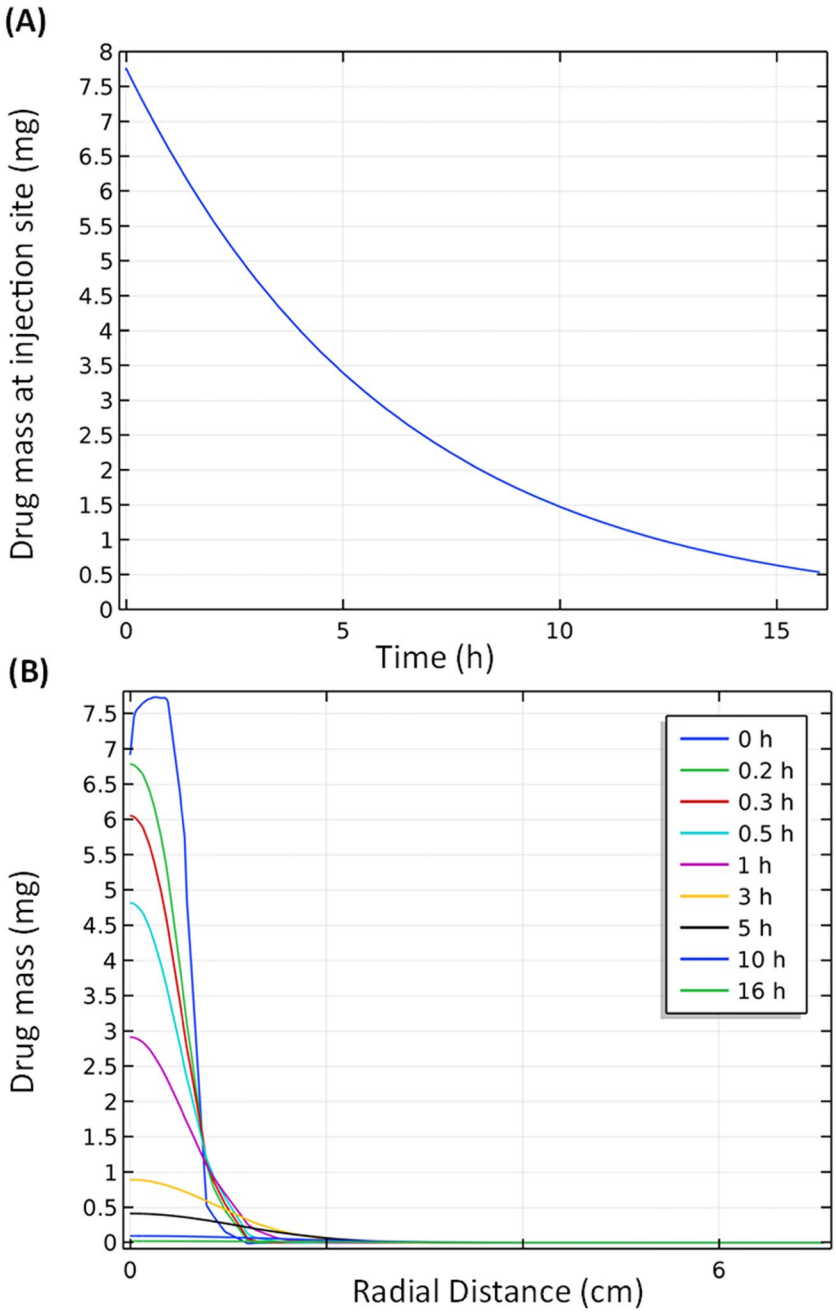

Fig. 10 Volume charts showing evolution of concentration of 7.5 mg SC dose for (**A**) injection process and (**B**) absorption process at MTX at a membrane permeability of 3.5×10^{-5} cm/s.

Figure 12D shows the effect on the plasma concentration profiles of MTX.

While changes in k_a were noted at all these conditions, only two conditions (pressure/hydraulic conductivity = 0 Pa/1×10^{-8} cm/(Pa*s) and 2000 Pa/1×10^{-8} cm/(Pa*s)) produced significant changes on the plasma concentration profiles. Both a pressure/hydraulic conductivity of 0 Pa/1×10^{-10} cm/(Pa*s) and 2000 Pa/1×10^{-10} cm/(Pa*s) were indistinguishable from each other, whereas 1133 Pa/1×10^{9} cm/(Pa*s) had a slight decrease in the C_{max}. These results suggest that hydraulic conductivity has a greater effect on absorption rates than pressure, however, there does appear to be a relationship between these two parameters. At high hydraulic conductivity, the effect on drug absorption and plasma concentration is very apparent, while moderate changes in both pressure and hydraulic conductivity appear to have a minimal effect. Since higher shear stress (related to higher fluid flow) can cause increased hydraulic conductivity *in vitro*, understanding this relationship in humans may be important to predict plasma drug concentration profiles for patients with high blood pressure.

The effect of diffusion rate from 6×10^{-8} to 6×10^{-4} cm^2/s on absorption rates was also tested at the higher membrane permeability rate and found to have a significant impact on

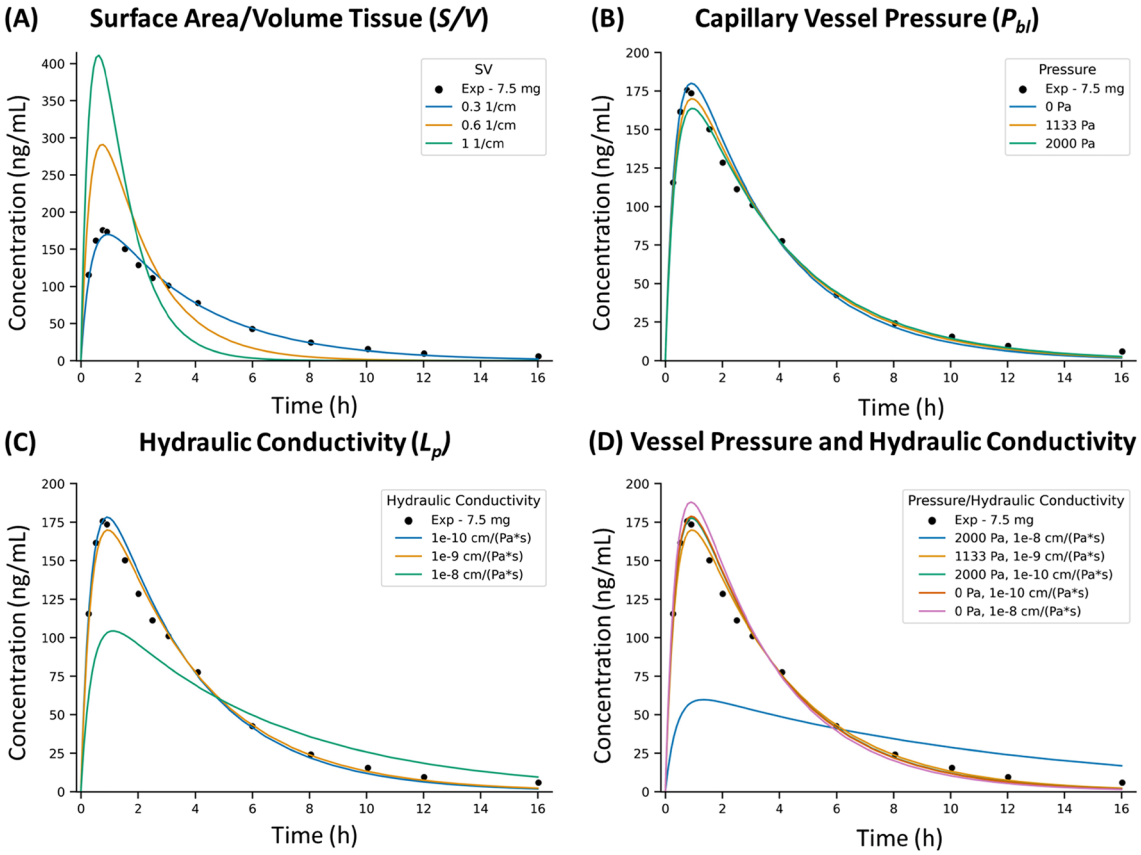

Fig. 11 Pharmacokinetic profiles of MTX with changes in capillary vessel physiology at high membrane permeability (3.5×10^{-5} cm/s): (**A**) surface area/tissue volume (S/V); (**B**) capillary vessel pressure (p_{bl}); (**C**) hydraulic conductivity (L_p); and (**D**) relationship between p_{bl} and L_p.

drug absorption and plasma concentration profiles (Fig. 12). Understanding the relationship between permeability and tissue diffusion may help in determining what kinds of *in vitro* tests should be implemented to develop better IVIVC. Table IV shows that as membrane permeability increases, the effect that diffusion rate has on absorption changes. It appears that for solubilized drugs injected SC, the diffusion rate will have the greatest effect on absorption rates for moderately permeable drugs (more permeable than BCS Class III or IV drugs, and less permeable than 1×10^{-4} cm/s). In this case, measuring the *in vivo* drug diffusion rate may help to improve *in vivo* plasma concentration predictions or correlations to humans. While some *in vitro* and *ex vivo* models exist for measuring drug diffusion rates in the skin [2, 31]. it is apparent that further implementation for measuring diffusion in the SC is important in correlating preclinical to clinical performance for solution injectables. For drugs with low membrane permeability, the sink condition is not fast enough for diffusion to have a significant impact.

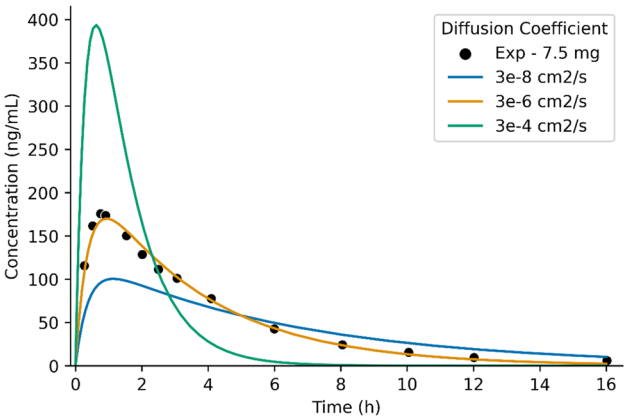

Fig. 12 Pharmacokinetic analysis of diffusion rate (D_{eff}) on MTX plasma concentrations.

Our results have also shown capillary blood vessel physiology can have a moderate effect on SC drug absorption.

Table V Effect of Pressure and Hydraulic Conductivity on Drug Absorption Rate

		P_{bl} (Pa)		
		0	**1133**	**2000**
L_p (cm/(Pa*s))	$\mathbf{1\times10^{-10}}$	0.315	--	0.311
	$\mathbf{1\times10^{-9}}$	--	0.295	--
	$\mathbf{1\times10^{-8}}$	0.334	--	0.0885

More so is the relationship between hydraulic conductivity and pressure, which have a slight synergistic effect on drug absorption rates. Therefore, incorporating local, SC capillary physiology into *in vitro* testing may help to greatly improve our understanding of SC administered drug pharmacokinetics. For example, the recently developed SCISSOR method has been validated for SC absorption of large molecules by simulating hydrodynamic pressure differences across an artificial membrane, without needing to model the complex physiological matrix [32]. For poorly permeable drugs (Class III or IV), these *in vitro* systems may be enough to adequately predict small molecule release and absorption given appropriate permeability models.

Our previous SC model showed that absorption of biologics – specifically, monoclonal antibodies (mAbs) – was highly dependent on diffusion rates [9]. Our current results show that for small molecules, membrane permeability is the rate determining factor. Reliable *in vitro* testing and/or estimations for this property is imperative to understanding not only the mechanism of drug absorption (e.g., passive vs. receptor-mediated transport) but also the potential impact that other factors, such as physiological variations, may have. In this study, literature values of MTX P_d from PAMPA models were insufficient to describe absorption rates, possibly due to receptor-mediated transport mechanisms of MTX absorption. In the absence of experimental data, some QSPR models [33] or estimations [17] have been used to predict membrane permeability. However, more accurate and accessible *in vitro* and *in silico* models, particularly those that can account for receptor-mediated transport, are needed.

Conclusion

In this study, a local SC absorption simulation model based on fluid physics was developed for small molecule capillary absorption. Vessel parameters, such as vessel pressure and hydraulic conductivity, were sourced from literature. Local absorption studies using methotrexate were further extended to predict SC pharmacokinetic profiles. Changes in injection site physiology had little impact on advective contribution to absorption; however, larger injection volumes may have greater effects. Membrane permeability was found to have the chief impact on solubilized small molecule absorption rates, in comparison to our previous study of mAb absorption rates where drug diffusion was the most important factor [9]. At higher membrane permeability, physiological parameters and diffusion had greater effects on drug absorption. The current results make it clear that appropriate permeability and diffusion models must be used for effective IVIVC and predictability of SC drug performance in humans. Our studies by sensitivity analyses offer additional understandings of how properties of, and interactions between, injected drug and the SC space can both contribute to systemic plasma concentrations of a solution formulated injectable. This model will be further expanded to include dissolution mechanisms of injected crystalline drug into the SC and better predict and formulate SC nanocrystalline long-acting injectables (LAI).

Acknowledgements We thank Allen Chao Endowment for supporting this research work.

Author Contributions CC drafted the manuscript, conducted simulations, and analyzed results. PH developed the simulation model. KP provided guidance of the research. TL directed the study and revised the manuscript.

Declarations

Conflict of Interests None.

References

1. Turner MR, Balu-Iyer S, v. Challenges and Opportunities for the Subcutaneous Delivery of Therapeutic Proteins. J Pharm Sci. 2018;107:1247–60.
2. Brohem CA, Cardeal LBD, Tiago M, Soengas MS, Barros SBD, Maria-Engler SS. Artificial skin in perspective: concepts and applications. Pigment Cell Melanoma Res. 2011;24:35–50.
3. Viola M, Sequeira J, Seica R, Veiga F, Serra J, Santos AC, Ribiero A. Subcutaneous delivery of monoclonal antibodies: How do we get there? J Control Release. 2018;286:301–14.
4. Mehta CH, Narayan R, Nayak UY. Computational modeling for formulation design. Drug Discov Today. 2019;24:781–8.
5. Zhao L, Tsakalozou E. The utility of in silico PBPK absorption modeling and simulation as a tool to develop bio-predictive dissolution methods. 2017. https://www.pharmacy.umaryland.edu/media/SOP/wwwpharmacyumarylandedu/centers/cersievents/dissolution/day2_hopi-lin.pdf. Accessed 8 Oct 2022.
6. Loisios-Konstantinidis I, Cristofoletti R, Fotaki N, Turner DB, Dressman J. Establishing virtual bioequivalence and clinically relevant specifications using in vitro 2 biorelevant dissolution testing and physiologically-based population pharmacokinetic modeling. Case example: Naproxen 4 5 6. Eur J Pharm Sci. 2020;143:105170.
7. Doki K, Darwich AS, Patel N, Rostami-Hodjegan A. Virtual bioequivalence for achlorhydric subjects: The use of PBPK modelling to assess the formulation-dependent effect of achlorhydria. Eur J Pharm Sci. 2017;109:111–20.
8. Rostami A. Virtual Bioequivalence (VBE) requirements for prudent use of PBPK in uncharted territories. (n.d.). https://www.fda.gov/media/138036/download. Accessed 15 Nov 2022.
9. Zheng F, Hou P, Corpstein CD, Xing L, Li T. Multiphysics Modeling and Simulation of Subcutaneous Injection and Absorption of Biotherapeutics: Model Development. Pharm Res. 2021;38:607–24.
10. Zheng F, Hou P, Corpstein CD, Park K, Li T. Multiscale pharmacokinetic modeling of systemic exposure of subcutaneously injected biotherapeutics. J Control Release. 2021;337:407–16.
11. Hou P, Zheng F, Corpstein CD, Xing L, Li T. Multiphysics Modeling and Simulation of Subcutaneous Injection and Absorption of Biotherapeutics: Sensitivity Analysis. Pharm Res. 2021;38:1011–30.
12. Scallan J, Huxley VH, Korthuis RJ. Capillary Fluid Exchange: Regulation, Functions, and Pathology. Integ Syst Physiol: from Mole Func Dis. 2010;2:1–94.
13. Fleischer S, Tavakol DN, Vunjak-Novakovic G. From Arteries to Capillaries: Approaches to Engineering Human Vasculature. Adv Funct Mater. 2020;30:1910811.

14. Gealekman O, Guseva N, Hartigan C, Apotheker S, Gorgoglione M, Gurav K, Tran K, Straubhaar J, Nicoloro S, Czech M, Thompson M, Perugini R, Corvera S. Depot-Specific Differences and Insufficient Subcutaneous Adipose Tissue Angiogenesis in Human Obesity. Circulation. 2011;123:186–94.
15. Mathura RA, Russell-Puleri S, Cancel LM, Tarbell JM. Hydraulic conductivity of endothelial cell-initiated arterial cocultures. Ann Biomed Eng. 2014;42:763–75.
16. Noddeland H. Influence of body posture on transcapillary pressures in human subcutaneous tissue. Scand J Clin Lab Invest. 1982;42:131–8.
17. Ibrahim R, Nitsche JM, Kasting GB, Scallan J, Huxley VH, Korthuis RJ. Dermal clearance model for epidermal bioavailability calculations. J Pharm Sci. 2010;101:2094–108.
18. DeMaio L, Tarbell JM, Scaduto RC, Gardner TW, Antonetti DA. A transmural pressure gradient induces mechanical and biological adaptive responses in endothelial cells. Am J Physiol Heart Circ Physiol. 2004;286:H731–41.
19. Sill HW, Chang YS, Artman JR, Frangos JA, Hollis TM, Tarbell JM. Shear stress increases hydraulic conductivity of cultured endothelial monolayers. Am J Phys. 1995;268(2 Pt 2):H535–43.
20. Schmidt D, Lynch J. Evaluation of the reproducibility of Parallel Artificial Membrane Permeation Assays (PAMPA). (n.d.). https://www.sigmaaldrich.com/US/en/technical-documents/technical-article/research-and-disease-areas/pharmacology-and-drug-discovery-research/evaluation-of-the-reproducibility-of-pampa. Accessed 8 Sep 2021.
21. Fort JJ, Shao Z, Mitra AK. Transport and degradation characteristics of methotrexate dialkyl ester prodrugs across tape-stripped hairless mouse skin. Int J Pharm. 1993;100:233–9.
22. Massironi SMG, Giacóia MR, Maiorka PC, Kipnis TL, Dagli MLZ. Skin morphology of the mutant hairless USP mouse. Braz J Med Biol Res. 2005;38:33–9.
23. Pichlmeier U, Heuer K-U. Subcutaneous administration of methotrexate with a prefilled autoinjector pen results in a higher relative bioavailability compared with oral administration of methotrexate. Clin Exp Rheumatol. 2014;32:563–71.
24. Le Merdy M, Mullin J, Lukacova V. Development of PBPK model for intra-articular injection in human: methotrexate solution and rheumatoid arthritis case study. J Pharmacokinet Pharmacodyn. 2021;48(6):909–22.
25. Halpern V, Combes SL, Dorflinger LJ, Weiner DH, Archer DF. Pharmacokinetics of subcutaneous depot medroxyprogesterone acetate injected in the upper arm. Contraception. 2014;89:31–5.
26. Michel CC. Capillary permeability and how it may change. J Physiol. 1988;404:1–29.
27. Rautio J, Kumpulainen H, Heimbach T, Oliyai R, Oh D, Järvinen T, Jouko S. Prodrugs: design and clinical applications. Nat Rev Drug Discov. 2008;7:255–70.
28. Fiehn C. Methotrexate transport mechanisms: the basis for targeted drug delivery and ß-folate-receptor-specific treatment. Clin Exp Rheumatol. 2010;28:S40–5.
29. McCabe MC, Hill RC, Calderone K, Cui Y, Yan Y, Quan T, Fisher G, Hansen K. Alterations in extracellular matrix composition during aging and photoaging of the skin. Matrix Biol Plus. 2020;8:100041.
30. Chen W, Yung BC, Qian ZY, Chen XY. Improving long-term subcutaneous drug delivery by regulating material-bioenvironment interaction. Adv Drug Deliv Rev. 2018;127:20–34.
31. Beissner N, Albero AB, Fuller J, Kellner T, Lauterboeck L, Liang JH, Bol M, Glasmacher B, Muller-Goymann C, Reichl S. Improved in vitro models for preclinical drug and formulation screening focusing on 2D and 3D skin and cornea constructs. Eur J Pharm Biopharm. 2018;126:57–66.
32. Kinnunen HM, Sharma V, Contreras-Rojas LR, Yu Y, Alleman C, Sreedhara A, Fischer S, Khawli L, Yohe S, Bumbaca D, Patapoff T, Daughterty A, Mrsny R. A novel in vitro method to model the fate of subcutaneously administered biopharmaceuticals and associated formulation components. J Control Release. 2015;214:94–102.
33. Bennion BJ, Be NA, McNerney MW, Lao V, Carlson EM, Valdez CA, Malfatti MA, Enright HA, Hguyen TH, Lightstone FC, Carpenter TS. Predicting a Drug's Membrane Permeability: A Computational Model Validated With in Vitro Permeability Assay Data. J Phys Chem. 2017;121(20):5228–37.